Available online at www.sciencedirect.com
SCIENCE DIRECT
Biochemical and Biophysical Research Communications 347 (2006) 76–82
BBRC
www.elsevier.com/locate/ybbrc

Silence of synaptotagmin I in INS-1 cells inhibits fast exocytosis and fast endocytosis

Xiong Xiong [a,1], Ke-Ming Zhou [a,1], Zheng-Xing Wu [a,*], Tao Xu [a,b,*]

[a] *Institute of Biophysics and Biochemistry, HuaZhong University of Science and Technology, Wuhan 430074, PR China*
[b] *National Laboratory of Biomacromolecules, Institute of Biophysics, Chinese Academy of Sciences, Beijing 100101, PR China*

Received 3 June 2006
Available online 16 June 2006

Abstract

Synaptotagmin I (Syt I) is a Ca^{2+} sensor for triggering fast synchronized release of neurotransmitters. However, controversy remains whether Syt I is also obligatory for the exocytosis and endocytosis of larger dense core vesicles (LDCVs) in endocrine cells. In this study, we used a short hairpin RNA (shRNA) to silence the expression of Syt I and investigated the roles of Syt I on exocytosis and endocytosis in INS-1 cells. Our results demonstrated that expression of Syt I is remarkably reduced by the Syt I gene targeting shRNA. Using high-time resolution capacitance measurement, we found that the silence of Syt I decreased the calcium sensitivity of fusion of insulin granules and therefore reduced the exocytotic burst triggered by step-like $[Ca^{2+}]_i$ elevation. In addition, the occurrence frequency and amplitude of fast endocytosis were remarkably reduced in the silenced cells. We conclude that Syt I not only participates in the Ca^{2+}-sensing of LDCV fusion with plasmalemma, but also plays a crucial role in fast endocytosis in INS-1 cells.

Keywords: INS-1 cell; Synaptotagmin I; shRNA; RNAi; Exocytosis; Endocytosis

Neurotransmitters and hormones are released by exocytosis, which was followed by endocytosis to take up the increased membrane for maintaining constant cellular volume[1,2]. Synaptotagmins, a large family of Ca^{2+}-binding proteins, are bewitching proteins, since cumulating evidence demonstrates that these proteins are Ca^{2+} sensors for vesicle fusion and play roles in endocytosis [3–6]. Until now, over fifteen isoforms of synaptotagmins have been identified in mammalian [7]. Among them, synaptotagmin I (Syt I) is best characterized as an abundant synaptic vesicle-associated protein which is evolutionarily conserved [8]. Syt I also exists on the large dense core vesicles (LDCVs) in neuroendocrine and endocrine cells [9–11].

Syt I functions as a Ca^{2+} sensor for the fast synchronous release of neurotransmitters in neurons from *Caenorhabditis elegans* to mammalian [8,12–15], as well as for exocytosis in chromaffin cells [9,16] and pituitary cells [10]. Changing the apparent Ca^{2+} affinity of Syt I causes an equivalent alteration in the Ca^{2+} dependence of release of transmitters [13,17,18]. In addition, Syt I is also involved in endocytosis [4,19–21] possibly by virtue of its interactions with dynamin and clathrin-associated adaptor molecules [22–26]. Synaptotagmin interacts with SNARE [soluble *N*-ethylmaleimide-sensitive fusion protein (NSF) attachment receptor] complex in Ca^{2+}-dependent or -independent way [27–30], and binds with phospholipids [31,32] to form minimal fusion machinery for at least the fast Ca^{2+}-dependent fusion of vesicles [33–36]. Synaptotagmin may also regulate the opening, closing, and dilation of fusion pore [37–40].

INS-1 cell line is derived from rat insulinoma and often used as a model cell for studying insulin secretion [41]. In the INS-1 cells, insulin was packed in LDCVs. Previous experiments show that Syt I does not express in primary β-cells [42–44], but Syt I and other isoforms including Syt V and IX are found expressed in INS-1 and other cell lines

* Corresponding authors. Fax: +86 10 64867566 (T. Xu), +86 27 87792024 (Z.-X. Wu).
E-mail addresses: xutao@ibp.ac.cn (Z.-X. Wu), ibbwuzx@mail.hust.edu.cn (T. Xu).
[1] These authors contributed equally to this work.

0006-291X/$ - see front matter © 2006 Elsevier Inc. All rights reserved.
doi:10.1016/j.bbrc.2006.06.045

derived from β-cell [45,46]. The role of Syt I in insulin secretion and endocytosis in INS-1 cell remains elusive. For verifying the function of Syt I in exocytosis and endocytosis in the INS-1 cells, we construct a plasmid encoding shRNA to silence Syt I gene. By employing high-time resolution capacitance measurement, we found that silence of Syt I not only reduced the exocytotic response to the step-like $[Ca^{2+}]_i$ elevation, but also reduced the occurrence and amplitude of the fast endocytosis.

Materials and methods

Materials. Anti-Syt I antibody was purchased from Santa Cruz Biotechnology (Santa Cruz, CA, USA). Quantum dots (Qdots) with maximum emission of 655 nm and Antibody Conjugation Kit were from Quantum dot Co. (Hayward, CA, USA). Most of reagents for Western blot, including HRP-conjugated rabbit anti-goat IgG, were purchased from Pierce Co. (Rockford, IL, USA). Restriction endonucleases, DNA ligase, and T4 polynucleotide kinase (PNK) were from New England Biolabs (Beverly, MA, USA). The mediums, fetal bovine serum (FBS), and other reagents for cell culture were from Gibco Co. (Carlsbad, CA, USA). Unless otherwise stated, other chemicals and reagents were purchased from Sigma–Aldrich Co. (St. Louis, MO, USA).

Construction of plasmids encoding shRNA. pRNAT-H1.1/Shuttle (H1.1) plasmid with a cGFP marker (Genescript, Scotch Plams, NJ, USA) was used as a vector for encoding shRNA *in vivo*. A 19-nucleotide target sequence of the rat synaptotagmin I gene (Accession No. X52772), GAG GAA AGA ACG CCA TTA A, was chosen according to the web-finder on Ambion website (http://www.ambion.com/) for construction of a Syt I-shRNA encoding plasmid (Syt I-sh) to silence the expression of Syt I. A random sequence of GCC ACA ACG TCT ATA TCA T was chosen as control shRNA (ctl-sh). Annealed double-stranded oligonucleotides encoding the target-sequence and the control shRNA were subcloned into the *Bam*H I–*Hin*dIII site of the H1.1 vector to generate the plasmids of Syt I-shRNA and ctl-shRNA. Construction integrity was verified by DNA sequencing provided by TaKaRa Co. (Dalian, China).

Cell culture and transfection. INS-1 cells were grown in RPMI 1640 supplemented with 10% (v/v) fetal bovine serum, 10 mM Hepes, 2 mM L-glutamine, 1 mM sodium pyruvate, and 50 mM 2-mercaptoethanol as described previously [41]. Cells were passaged at about 1:3 by treatment of trypsin/EDTA every 3 days. Cells cultured for 24 h were transfected by the Syt I-shRNA and ctl-shRNA plasmids, respectively, with Lipofectamine 2000 (Life Technologies, Grand Island, NY, USA) per the manufacturer's protocol. In addition, an insulin-EGFP chimera encoding plasmid was used to transfect INS-1 cell for identification of insulin-containing granules. All experiments were performed at room temperature. The transfected cells were identified by the presence of green fluorescence excited by illumination of 488 nm light from a monochromator (Polychrome IV, Till Photonics, Planegg, Germany).

Conjugation of Qdots with IgG. The Qdots were conjugated with anti-Syt I-IgG using Qdot Antibody Conjugation Kit as described in the user's manual to generate an anti-Syt I-Qdot as a fluorescence probe for Syt I in immunocytochemistry.

Western blot analysis and immunofluorescence imaging. For Western blotting, the cells transfected with Syt I-shRNA and ctl-shRNA plasmids for 48 h were sorted and collected by FACS (fluorescence-activated cell sorter). Total cell protein extracts were prepared by lysing cells with M-PER mammalian protein extraction reagent kit supplemented with 86 μg/ml PMSF, 50 μg/ml aprotinin, and 5 μg/ml leupeptin (Roche, Basel, Switzerland). Western blot analysis was performed as described previously [47]. Briefly, primary antibody, goat anti-Syt I-IgG, diluted 1:1000; and second antibody, HRP-conjugated rabbit anti-goat IgG, diluted 1:10,000 in blocking buffer. Developed X-films were scanned into computer, and the bands were quantified by CorelDRAW 9 (Corel Co., Eden Prairie, MN, USA).

For immunofluorescence imaging, the transfected cells were re-plated on coverslips and fixed 1 day later with 4% paraformaldehyde in PBS for 20 min. The cells were permeabilized and blocked for 10 min with 1% Triton X-100 and 3% BSA in PBS, and incubated with anti-Syt I-Qdots in blocking buffer for 2 h. The cells were washed five times with PBS and then mounted with 90% glycerol. Insulin-EGFP plasmid transfected cells were used for identifying the co-localization of insulin-containing granules and Syt I, and Syt I-shRNA plasmid transfected cells were used to detect the silence effect. Immunofluorescence imaging was performed with wild field and total internal reflection fluorescence microscope (TIRFM) system as previously described [48]. An additional Micro-Imager DUAL-View (Optical Insights, Dodge-Blvd, Tucson, AZ, USA) was used for dual image acquisition of fluorescence emitted from GFPs and Qdots. Both GFPs and Qdots were excited by 488 nm light.

Membrane capacitance (C_m) measurement. The C_m of INS-1 cells were measured in real time using an EPC10 amplifier (Heka Electronics, Lambrecht, Germany) in conventional whole-cell patch clamp configuration. A sine + DC protocol was applied using the Lockin extension of the Pulse program (Heka Electronics). The cells were voltage clamped at a holding potential of −70 mV and a sine wave voltage command with amplitude of 20 mV and frequency of 1042 Hz was applied. Currents were filtered at 2.9 kHz and sampled at 25 kHz. The normal bath solution contained (in mM): 138 NaCl, 5.6 KCl, 2.6 $CaCl_2$, 1.2 $MgCl_2$, 5 Hepes, and 3 glucose (adjusted to pH 7.4 with NaOH, 310 mOsm).

Ca^{2+}-uncaging and $[Ca^{2+}]_i$ measurement. Homogeneous global $[Ca^{2+}]_i$ elevation was generated by photolysis of the caged-Ca^{2+} compound, 1-(4,5-dimethoxy-2-nitrophenyl)-1,2-diaminoethane-*N*,*N*,*N*′,*N*′-tetraacetic acid (DMNP-EDTA, Molecular Probes, Carlsbad, CA, USA), with UV light sourced as previously described [49]. The DMNP-EDTA containing pipette solution contained (in mM): 110 CsGlu, 5 DMNP-EDTA, 8 NaCl, 3.6 $CaCl_2$, 2 MgATP, 0.3 GTP, 0.2 fura-6F or 0.2 mag-fura 2, and 35 Hepes, adjusted to pH 7.2 using CsOH or HCl (osmolarity, 300 mOsm). The free Ca^{2+} concentration of the pipette solution was determined to be around 200 nM.

Post-flash $[Ca^{2+}]_i$ in a flash photolysis experiment in which the step-like $[Ca^{2+}]_i$ elevation was elicited by UV flash generated from a Rapp flash lamp (Rapp Optoelektronik, Hamburg, Germany) was measured using dual wavelength excitation method as suggested by Grynkiewicz et al. [50]. The flash was followed by a series of illuminations alternating between 350 and 380 nm which were generated from the monochromator (Polychrome IV, Till Photonics) and allowed ratiometric determination of the Ca^{2+} concentration according to the equation: $[Ca^{2+}]_i = K_{eff} \times (R - R_{min})/(R_{max} - R)$ [50], where K_{eff}, R_{min}, and R_{max} are constants obtained from *in vivo* calibration. The duration of these illuminations was adjusted to maintain relatively constant Ca^{2+} concentrations, since the illumination at 350 and 380 nm also led to photolytic release of Ca^{2+}. The resulting fluorescence was acquired by a photodiode (Till Photonics).

Datum analysis. Analysis of capacitance data was performed in IGOR Pro 4.02 (WaveMetrics, Lake Oswego, OR), and results were presented as means ± SEM with the indicated number of experiments. Statistical significance was evaluated by Student's *t* test or Mann–Whitney Rank Sum test according to the normality of datum distribution in SigmaStat 3.11 (Systat Software, Inc., Canal Blvd., Suite C Richmond, CA, USA). A value of $P < 0.05$ was considered to be statistically significant. The Ca^{2+} dependence of exocytosis is examined by plotting the rate constant, which was obtained by fitting the exocytotic burst with exponential function, versus $[Ca^{2+}]_i$ on a double logarithmic scale.

Results

Syt I is present on insulin granules of INS-1 cells and is knocked down by Syt I-shRNA

INS-1 cell line is derived from a rat insulinoma. Previous report has shown that Syt I is not detected in primary rat pancreas β-cells [42–44], so it is important to verify the

existence of Syt I in INS-1 cells. We detected abundant presence of Syt I-mRNA in INS-1 cells using RT-PCR (data not shown). To confirm the expression and localization of Syt I, we employed immunocytochemistry assay with the anti-Syt I-Qdots. Syt I was detected in the INS-1 cells as fluorescent spots and co-localized well with the EGFP-insulin labeling granules as shown in Fig. 1. The result demonstrated that Syt I expressed on the insulin-containing granules.

To silence the expression of Syt I in INS-1 cells, we constructed a Syt I-shRNA plasmid which encodes a Syt I gene-target shRNA and a cGFP marker, and used it to transfected INS-1 cells. The transfected cells were identified by the presence of green fluorescence illuminated by 488 nm light. The silencing effect of Syt I-shRNA plasmid was estimated by immunocytochemistry and Western blot. Immunocytochemistry assay showed that the expression of Syt I was reduced to a very low level but not abolished in the transfected cells as displayed in Fig. 2. The result was further confirmed by Western blot as shown in Fig. 3A and B. The silence efficiency of Syt I-sh plasmids was ~80% (79.6 ± 3.31, $n = 5$). The knockdown of Syt I was not due to the transfection itself, since transfection of ctl-sh plasmid, which encodes a random shRNA, had no significant effect on expression level of Syt I (Fig. 3B).

The silence of Syt I reduces the exocytotic burst by decreasing the Ca^{2+}-sensitivities of fusion in INS-1 cells

Syt I was reported as a Ca^{2+} sensor for exocytotic fast burst in chromaffin cell [9,10]. For detecting the exocytotic effect of Syt I in INS-1 cells, we employed high time resolution capacitance measurement in whole cell model to measure the secretory response to step-like calcium elevation photolysed by a flash of strong UV light in the wild type and Syt I-shRNA encoding plasmid transfected cells. The silenced cells exhibited significant smaller exocytotic burst comparing with wild-type cells as a control (Fig. 4A, bottom panel), albeit the triggering calcium signals were almost the same (Fig. 4A, upper panel). The summarized data showed that the bursts in control and transfected cells were 217 ± 18 fF ($n = 28$) and 137 ± 16 fF ($n = 31$), respectively, which shows significant difference ($P < 0.01$) analyzed by Mann–Whitney rank sum test (Fig. 4B), suggesting that Syt I is a calcium sensor for exocytotic burst in INS-1 cells. For probing into the mechanism underlying the regulative effect of Syt I, we fitted the exocytotic burst curve with exponential function to analyze its dynamics. As shown in Fig. 4C, the rate constant of exocytotic burst in silenced cells ($6.23 \pm 1.09\ s^{-1}$) was significantly slower ($P < 0.01$) than that in control cells

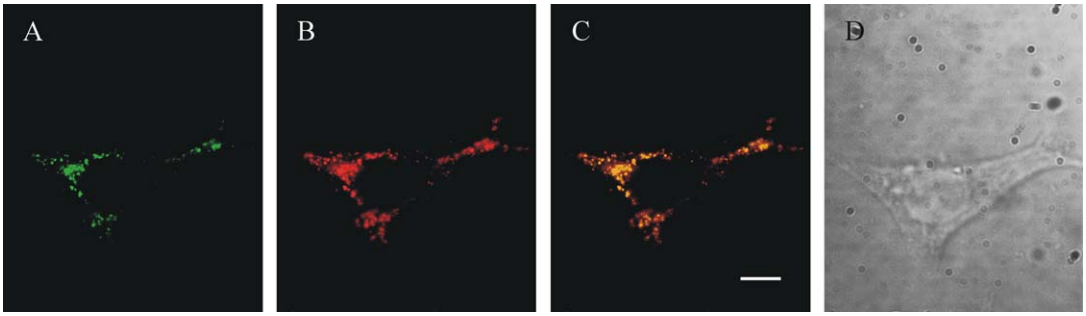

Fig. 1. Syt I co-localizes with insulin-containing granules in INS-1 cells. After INS-1 cells were transfected with expression vector encoding EGFP-tagged insulin, they were fixed with paraformaldehyde and immunostained with anti-Syt I-Qdots as described under Materials and methods. The cells were imaged under wild field fluorescence microscope. (A) Image of EGFP-insulin in green channel. (B) Image of anti-Syt I-Qdots in red channel. (C) The merged image of (A) and (B) displays a significant overlap (yellow) of the EGFP-insulin (green) and anti-Syt I-Qdots (red) fluorescence. (D) Transmission image of the cell at the same focus plane as (A) and (B). Scale bar: 10 μm. (For interpretation of the references to color in this figure legend, the reader is referred to the web version of this paper.)

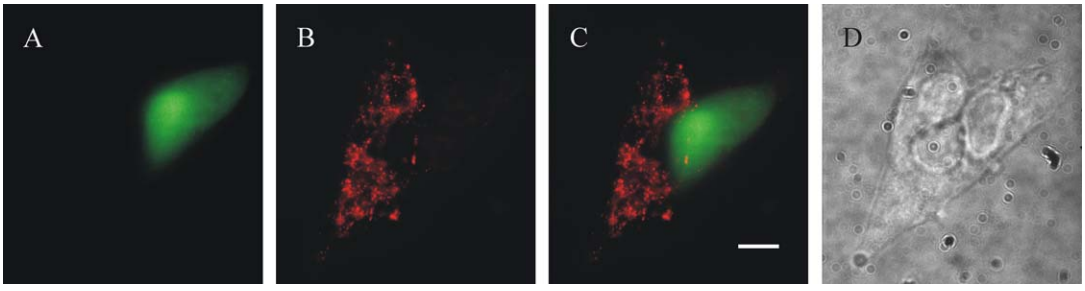

Fig. 2. Immunofluorescence assay of Syt I expression levels in wild type and Syt I-silenced cells. The wild type and Syt I-sh-transfected (green) cells were immunostained with anti-Syt I-Qdots and imaged under wild field fluorescence microscope as described in Fig. 1. (A) Image of Syt I-sh transfected cell in green channel. (B) Image of cell immunostained with anti-Syt I Qdots in red channel. (C) Overlay of (A) and (B) clearly showed that the expression level of Syt I in the SytI-sh transfected cell is much less than that in the wild type cell. (D) Transmission image of the same cells. Scale bar: 10 μm. (For interpretation of the references to color in this figure legend, the reader is referred to the web version of this paper.)

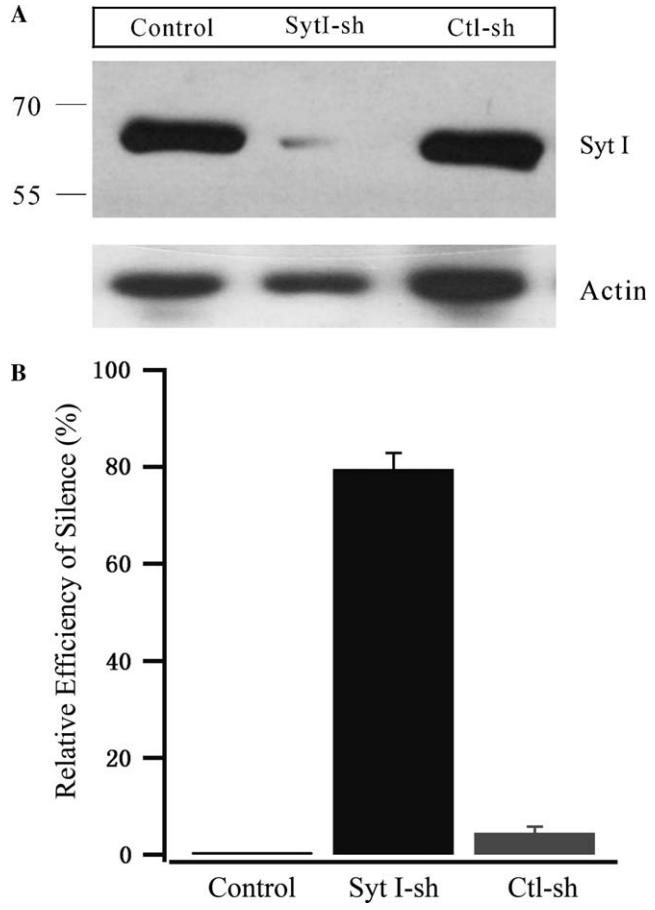

Fig. 3. Selective Reduction of Syt I expression in INS-1 cells by shRNA. (A) Expression level of Syt I analyzed by Western blotting using anti-Syt I IgG in wild type cells (control), Syt I-sh transfected cells (Syt I-sh) and the cells transfected with ctl-sh plasmid encoding a random sequence of RNA. Actin was chosen as a loading control and detected by anti-actin IgG. (B) Summary of the expression level of Syt I in the wild type cells (control) and cells transfected with Syt I-sh plasmids (Syt I-sh, black bar) and ctl-sh plasmids (ctl-sh, gray bar). The relative efficiency of silence was calculated using the formula: $E_s = (1 - bc/ad) \times 100\%$, where E_s is the relative efficiency of the silence; a and b represent quantities of Syt I in the control cells and Syt I-sh transfected cells; c and d, actin level from control and Syt I-sh transfected cells, respectively.

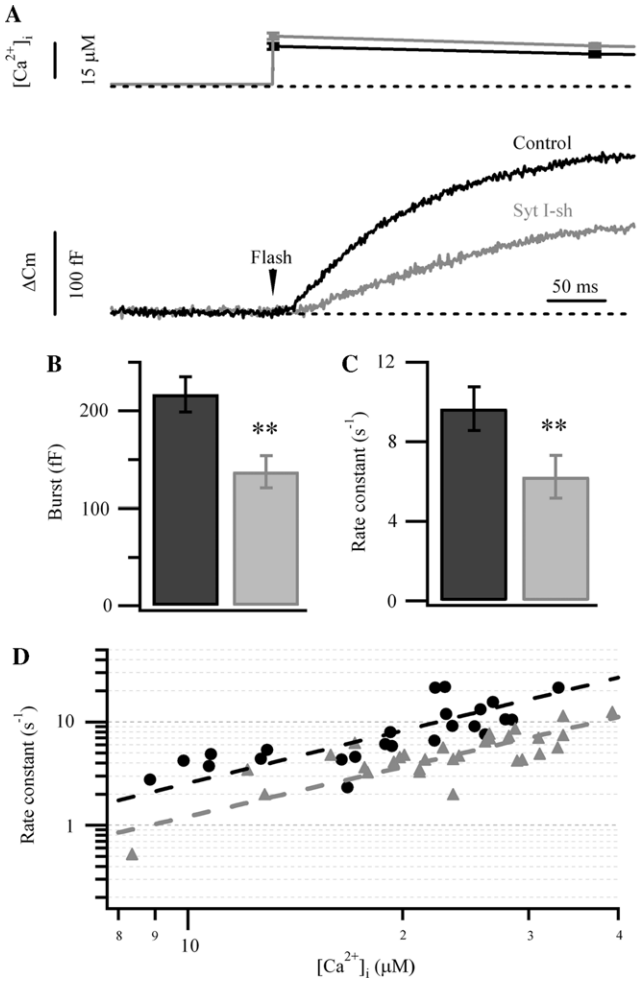

Fig. 4. Silence of Syt I expression attenuated exocytosis in INS-1 cells by decreasing the Ca^{2+}-sensitivity of secretion. (A) The exocytotic burst measured by high time resolution C_m measurement in wild type cells (control, black trace) and Syt I knockdown cells (Syt I-sh, gray trace) in response to step-like $[Ca^{2+}]_i$ elevation generated by flash photolysis of caged-Ca^{2+} (upper panel). (B) The amplitude of the exocytotic burst in the knockdown cells (gray bar) was significantly reduced as compared to that of control cells (black bar). (C) Rate constant of the exocytotic burst in the silenced cells was also reduced remarkably as compared to that of control cells. (D) The silence of Syt I expression decreased Ca^{2+} sensitivity but had no significant effect on the Ca^{2+} cooperativity of fusion. $^{**}P < 0.01$.

$(9.67 \pm 1.11\ s^{-1})$. By plotting the rate constants of exocytotic burst versus the post-flash $[Ca^{2+}]_i$ on a double logarithmic scale, we get its Ca^{2+}-dependence [51] as shown in Fig. 4D. The silenced cells displayed lower Ca^{2+}-sensitivities of fusion comparing with the control cells (indicated by the y-intercept of the power function-fitted curves), albeit the Ca^{2+}-cooperativities remained unchanged as indicated by the slopes of the fitted curves. The results demonstrated that the knockdown of Syt I reduces calcium sensitivity of exocytosis in INS-1 cells and thereby decreases insulin secretion.

Syt I plays an important role in the fast endocytosis in INS-1 cells

Secretion needs a balance between of vesicle exocytosis and endocytosis to make homeostasis of cell volume. In wild-type INS-1 cells, exocytosis is frequently accompanied by endocytosis about 300 ms later (23 events out of 28 control cells and 26 events/31 silenced cells). In flash experiments, there were two types of distinct endocytosis. The first type (1st type endocytosis) in which there existed both fast and slow endocytotic components is best fitted with double exponential function. The second one (2nd type endocytosis), there existed only slow kinetic component of endocytosis which was best fitted with single exponential function. The phenomenon was also observed in primary rat pancreatic β cells (data not shown). The total amplitude of endocytosis was measured from the time of onset of endocytosis (the cross-point of exponential function fitted trace of exocytotic curve and endocytotic trace) to end of measurement. The amplitude of fast exocytotic component was

obtained from exponential function fit. The endocytotic maximum rate $[(-\Delta C_m/\Delta t)_{max}]$ was estimated by dividing the decrement of C_m at time $= \tau/2$ by Δt (from the time of onset of endocytosis to time $= \tau/2$), where τ is the time constant (reciprocal of rate constant) from the single exponential fit of the 2nd type endocytosis or the time constant of fast endocytotic component from the double exponential fit to the 1st type endocytosis.

Surprisingly, we found that Syt I silence also reduced endocytosis. As shown in Fig. 5B, averaged total endocytosis was reduced from 396 ± 79 fF in the control cells to 207 ± 58 fF in the silenced cells. Further analysis of the kinetic components found that the amplitude of the fast endocytosis was preferentially reduced, whereas the slow one remained unaffected. The amplitudes of the fast endocytosis in the control cells and the Syt I-silenced cells were 435 ± 104 fF ($n = 12$) and 133 ± 15 fF ($n = 4$), and those of the slow endocytosis were 169 ± 32 fF ($n = 23$) and 186 ± 57 fF ($n = 26$), respectively. The rate constants of the slow endocytosis in the knockdown cells ($3.19 \pm 1.19\ s^{-1}$, $n = 26$) were not significantly different from those of the control cells ($3.03 \pm 0.49\ s^{-1}$, $n = 23$). As summarized in Fig. 5D, the knockdown of Syt I reduced the maximum rate of endocytosis from 516 ± 135 fF/s ($n = 23$) in control cells to 106 ± 31 fF/s ($n = 26$) in the silenced cells. We further analyzed the occurrence frequency of fast endocytosis in the cells displaying endocytosis. Among all the endocytotic events, about 52% showed fast endocytosis in control cells, this percentage was dramatically decreased to 15% in the Syt I-knockeddown cells (Fig. 5E). These results suggest Syt I is involved in both exocytosis and fast endocytosis.

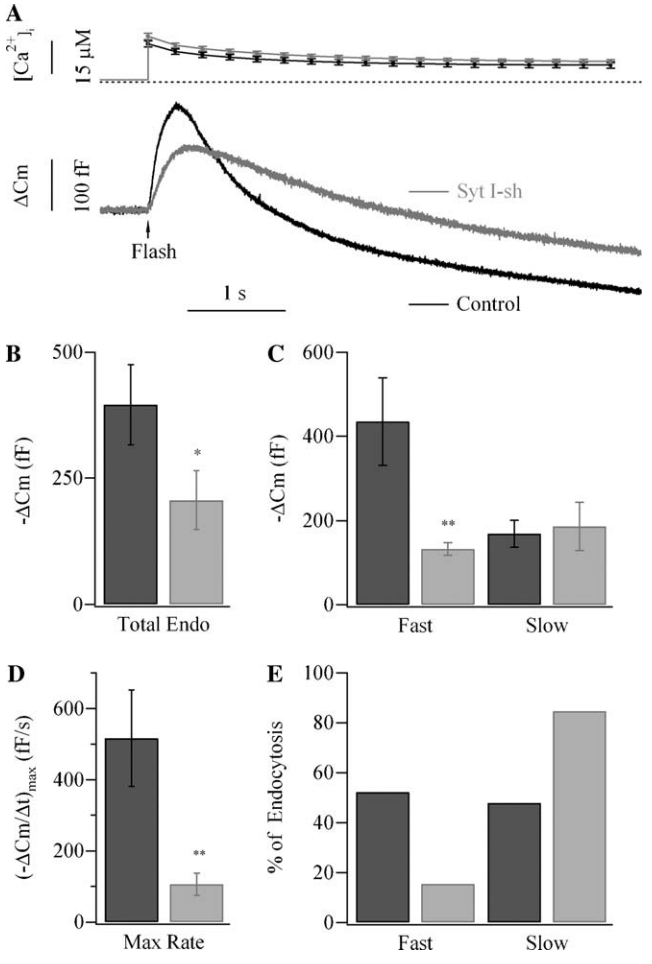

Fig. 5. Silence of Syt I expression selectively inhibited the fast endocytosis in INS-1 cells. (A) The exocytotic response (bottom panel) to the flash stimuli (upper panel) in INS-1 cells was frequently followed by endocytosis. The silence of Syt I (gray curve, Syt I-sh) reduced the fast endocytosis in INS-1 cells as compared with control cells (control, black trace). (B, C, and D) The knockdown of Syt I (gray bar) significantly reduced the total amplitude of endocytosis (B), selectively decreased the fast endocytotic amplitude without affecting the slow endocytosis (C), and reduced the maximum endocytotic rate (D), as compared with those of control cells (black bar). (E) The reduction of Syt I expression decreased the occurring frequency of fast endocytosis and increased the percentage of slow endocytosis from all the cells that exhibiting endocytosis. $^*P < 0.05$; $^{**}P < 0.01$.

Discussion

The Ca^{2+} sensor for insulin secretion is controversial [42,43,45,52]. Here we studied the role of Syt I in insulin secretion from a rat insulinoma cell line, INS-1 [41]. Our immunocytochemistry experiment demonstrated the expression of Syt I on insulin-containing granules in INS-1 cells. By transfecting the INS-1 cells with a plasmid encoding a shRNA which targets a specific sequence of Syt I mRNA, expression of Syt I protein is specifically knocked down. The advantages of RNA interference technique include lack of developmental problems and lethality, relative ease, rapidness, and lower cost comparing with gene knockout.

We show that knock down of Syt I reduces both the amplitude and maximum rate of exocytosis stimulated by a step-like $[Ca^{2+}]_i$ elevation. Analysis of the Ca^{2+}-dependence of fusion demonstrates that the Ca^{2+}-sensitivity is decreased but the Ca^{2+}-cooperativity remains unchanged by silencing Syt I. The result confirms that the Ca^{2+}-sensing role of Syt I in LDCV fusion [9,11,17,53]. Although Syt I is not detected in primary pancreatic β cells [42–44], it is found abundantly expressed in INS-1 cells [45,46]. While confirming the essential role of Syt I in insulin secretion from INS-1 cells, the physiological function of Syt I in insulin release remains unclear. It is possible that the expression of Syt I in primary β cells is too low to be detected. However, the low abundance of Syt I does not necessarily indicate that Syt I is not involved in insulin secretion under physiological condition. Or it is likely that Syt I expression is only unregulated in insulinoma cell line, implying that caution should be taken when extrapolating the conclusion from cell line study to primary tissues.

Endocytosis is an important cellular process, by which the increased plasma membrane is taken up into cell, and the released vesicles are renewed and reused. Fast and slow modes of endocytosis are found to co-exist at a number of synapses and in various cells. Our high-time resolution

capacitance measurement shows that the occurrence and amplitude of fast endocytotic events are inhibited by the knock down of Syt I. The fast endocytosis is characterized by a very fast endocytotic rate $\frac{1}{\tau} > 1s^{-1}$ and an amplitude normally exceeding that of exocytosis [54,55]. It has been reported that a certain threshold is required to induce the fast endocytosis [54–56]. Up to now, the molecular mechanism and physiological significance of the fast endocytosis remain elusive. Our result that Syt I is required for the fast endocytosis in INS-1 cells will help to elucidate the molecular requirements of the fast endocytosis.

Acknowledgments

This work was supported by grants from the National Science Foundation of China (30270363, 30470448, and 30470646), the Major State Basic Research Program of PR China (2004CB720000), the CAS Project (KSCX2-SW-224), the Li Foundation, and the Sino-German Scientific Center. The laboratory of T.X. belongs to a Partner Group Scheme of the Max Planck Institute for Biophysical Chemistry, Göttingen.

References

[1] R. Jahn, T. Lang, T.C. Sudhof, Membrane fusion, Cell 112 (2003) 519–533.
[2] T.C. Sudhof, The synaptic vesicle cycle, Annu. Rev. Neurosci. 27 (2004) 509–547.
[3] E.R. Chapman, Synaptotagmin: a Ca^{2+} sensor that triggers exocytosis? Nat. Rev. Mol. Cell Biol. 3 (2002) 498–508.
[4] E.M. Jorgensen, E. Hartwieg, K. Schuske, M.L. Nonet, Y. Jin, H.R. Horvitz, Defective recycling of synaptic vesicles in synaptotagmin mutants of *Caenorhabditis elegans*, Nature 378 (1995) 196–199.
[5] K.E. Poskanzer, K.W. Marek, S.T. Sweeney, G.W. Davis, Synaptotagmin I is necessary for compensatory synaptic vesicle endocytosis in vivo, Nature 426 (2003) 559–563.
[6] T.L. Schwarz, Synaptotagmin promotes both vesicle fusion and recycling, Proc. Natl. Acad. Sci. USA 101 (2004) 16401–16402.
[7] M. Craxton, Synaptotagmin gene content of the sequenced genomes, BMC Genomics 5 (2004) 43.
[8] M. Geppert, Y. Goda, R.E. Hammer, C. Li, T.W. Rosahl, C.F. Stevens, T.C. Sudhof, Synaptotagmin I: a major Ca^{2+} sensor for transmitter release at a central synapse, Cell 79 (1994) 717–727.
[9] T. Voets, T. Moser, P.E. Lund, R.H. Chow, M. Geppert, T.C. Sudhof, E. Neher, Intracellular calcium dependence of large dense-core vesicle exocytosis in the absence of synaptotagmin I, Proc. Natl. Acad. Sci. USA 98 (2001) 11680–11685.
[10] M. Kreft, V. Kuster, S. Grilc, M. Rupnik, I. Milisav, R. Zorec, Synaptotagmin I increases the probability of vesicle fusion at low Ca^{2+} in pituitary cells, Am. J. Physiol. Cell Physiol. 284 (2003) C547–C554.
[11] G.W. Lawrence, J.O. Dolly, Ca^{2+}-induced changes in SNAREs and synaptotagmin I correlate with triggered exocytosis from chromaffin cells: insights gleaned into the signal transduction using trypsin and botulinum toxins, J. Cell Sci. 115 (2002) 2791–2800.
[12] A. DiAntonio, K.D. Parfitt, T.L. Schwarz, Synaptic transmission persists in synaptotagmin mutants of *Drosophila*, Cell 73 (1993) 1281–1290.
[13] R. Fernandez-Chacon, A. Konigstorfer, S.H. Gerber, J. Garcia, M.F. Matos, C.F. Stevens, N. Brose, J. Rizo, C. Rosenmund, T.C. Sudhof, Synaptotagmin I functions as a calcium regulator of release probability, Nature 410 (2001) 41–49.
[14] M.L. Nonet, K. Grundahl, B.J. Meyer, J.B. Rand, Synaptic function is impaired but not eliminated in *C. elegans* mutants lacking synaptotagmin, Cell 73 (1993) 1291–1305.
[15] M. Yoshihara, J.T. Littleton, Synaptotagmin I functions as a calcium sensor to synchronize neurotransmitter release, Neuron 36 (2002) 897–908.
[16] O.H. Shin, J. Rizo, T.C. Sudhof, Synaptotagmin function in dense core vesicle exocytosis studied in cracked PC12 cells, Nat. Neurosci. 5 (2002) 649–656.
[17] J.B. Sorensen, R. Fernandez-Chacon, T.C. Sudhof, E. Neher, Examining synaptotagmin 1 function in dense core vesicle exocytosis under direct control of Ca^{2+}, J. Gen. Physiol. 122 (2003) 265–276.
[18] J.S. Rhee, L.Y. Li, O.H. Shin, J.C. Rah, J. Rizo, T.C. Sudhof, C. Rosenmund, Augmenting neurotransmitter release by enhancing the apparent Ca^{2+} affinity of synaptotagmin 1, Proc. Natl. Acad. Sci. USA 102 (2005) 18664–18669.
[19] J.T. Littleton, J. Bai, B. Vyas, R. Desai, A.E. Baltus, M.B. Garment, S.D. Carlson, B. Ganetzky, E.R. Chapman, Synaptotagmin mutants reveal essential functions for the C2B domain in Ca^{2+}-triggered fusion and recycling of synaptic vesicles in vivo, J. Neurosci. 21 (2001) 1421–1433.
[20] K. Nicholson-Tomishima, T.A. Ryan, Kinetic efficiency of endocytosis at mammalian CNS synapses requires synaptotagmin I, Proc. Natl. Acad. Sci. USA 101 (2004) 16648–16652.
[21] K.E. Poskanzer, K.W. Marek, S.T. Sweeney, G.W. Davis, Synaptotagmin I is necessary for compensatory synaptic vesicle endocytosis in vivo, Nature 426 (2003) 559–563.
[22] J.Z. Zhang, B.A. Davletov, T.C. Sudhof, R.G. Anderson, Synaptotagmin I is a high affinity receptor for clathrin AP-2: implications for membrane recycling, Cell 78 (1994) 751–760.
[23] V. Haucke, P. De Camilli, AP-2 recruitment to synaptotagmin stimulated by tyrosine-based endocytic motifs, Science 285 (1999) 1268–1271.
[24] N. Jarousse, R.B. Kelly, The AP2 binding site of synaptotagmin 1 is not an internalization signal but a regulator of endocytosis, J. Cell Biol. 154 (2001) 857–866.
[25] E.R. Chapman, R.C. Desai, A.F. Davis, C.K. Tornehl, Delineation of the oligomerization, AP-2 binding, and synprint binding region of the C2B domain of synaptotagmin, J. Biol. Chem. 273 (1998) 32966–32972.
[26] M.E. Graham, D.W. O'Callaghan, H.T. McMahon, R.D. Burgoyne, Dynamin-dependent and dynamin-independent processes contribute to the regulation of single vesicle release kinetics and quantal size, Proc. Natl. Acad. Sci. USA 99 (2002) 7124–7129.
[27] C. Rickman, B. Davletov, Mechanism of calcium-independent synaptotagmin binding to target SNAREs, J. Biol. Chem. 278 (2003) 5501–5504.
[28] X. Shao, C. Li, I. Fernandez, X. Zhang, T.C. Sudhof, J. Rizo, Synaptotagmin-syntaxin interaction: the C2 domain as a Ca^{2+}-dependent electrostatic switch, Neuron 18 (1997) 133–142.
[29] J.A. Ernst, A.T. Brunger, High resolution structure, stability, and synaptotagmin binding of a truncated neuronal SNARE complex, J. Biol. Chem. 278 (2003) 8630–8636.
[30] M.E. Bowen, K. Weninger, J. Ernst, S. Chu, A.T. Brunger, Single-molecule studies of synaptotagmin and complexin binding to the SNARE complex, Biophys. J. 89 (2005) 690–702.
[31] J. Bai, W.C. Tucker, E.R. Chapman, PIP_2 increases the speed of response of synaptotagmin and steers its membrane-penetration activity toward the plasma membrane, Nat. Struct. Mol. Biol. 11 (2004) 36–44.
[32] D. Arac, X. Chen, H.A. Khant, J. Ubach, S.J. Ludtke, M. Kikkawa, A.E. Johnson, W. Chiu, T.C. Sudhof, J. Rizo, Close membrane-membrane proximity induced by Ca^{2+}-dependent multivalent binding of synaptotagmin-1 to phospholipids, Nat. Struct. Mol. Biol. 13 (2006) 209–217.
[33] X. Zhang, M.J. Kim-Miller, M. Fukuda, J.A. Kowalchyk, T.F. Martin, Ca^{2+}-dependent synaptotagmin binding to SNAP-25 is essential for Ca^{2+}-triggered exocytosis, Neuron 34 (2002) 599–611.

[34] W.C. Tucker, T. Weber, E.R. Chapman, Reconstitution of Ca^{2+}-regulated membrane fusion by synaptotagmin and SNAREs, Science 304 (2004) 435–438.
[35] G. Schiavo, G. Stenbeck, J.E. Rothman, T.H. Sollner, Binding of the synaptic vesicle v-SNARE, synaptotagmin, to the plasma membrane t-SNARE, SNAP-25, can explain docked vesicles at neurotoxin-treated synapses, Proc. Natl. Acad. Sci. USA 94 (1997) 997–1001.
[36] A. Bhalla, M.C. Chicka, W.C. Tucker, E.R. Chapman, Ca^{2+}-synaptotagmin directly regulates t-SNARE function during reconstituted membrane fusion, Nat. Struct. Mol. Biol. (2006).
[37] J. Bai, C.T. Wang, D.A. Richards, M.B. Jackson, E.R. Chapman, Fusion pore dynamics are regulated by synaptotagmin*t-SNARE interactions, Neuron 41 (2004) 929–942.
[38] J.K. Jaiswal, S. Chakrabarti, N.W. Andrews, S.M. Simon, Synaptotagmin VII restricts fusion pore expansion during lysosomal exocytosis, PLoS Biol. 2 (2004) E233.
[39] C.T. Wang, J. Bai, P.Y. Chang, E.R. Chapman, M.B. Jackson, Synaptotagmin-Ca^{2+} triggers two sequential steps in regulated exocytosis in rat PC12 cells: fusion pore opening and fusion pore dilation, J. Physiol. 570 (2006) 295–307.
[40] C.T. Wang, R. Grishanin, C.A. Earles, P.Y. Chang, T.F. Martin, E.R. Chapman, M.B. Jackson, Synaptotagmin modulation of fusion pore kinetics in regulated exocytosis of dense-core vesicles, Science 294 (2001) 1111–1115.
[41] M. Asfari, D. Janjic, P. Meda, G. Li, P.A. Halban, C.B. Wollheim, Establishment of 2-mercaptoethanol-dependent differentiated insulin-secreting cell lines, Endocrinology 130 (1992) 167–178.
[42] Z. Gao, J. Reavey-Cantwell, R.A. Young, P. Jegier, B.A. Wolf, Synaptotagmin III/VII isoforms mediate Ca^{2+}-induced insulin secretion in pancreatic islet β-cells, J. Biol. Chem. 275 (2000) 36079–36085.
[43] H. Brown, B. Meister, J. Deeney, B.E. Corkey, S.N. Yang, O. Larsson, C.J. Rhodes, S. Seino, P.O. Berggren, G. Fried, Synaptotagmin III isoform is compartmentalized in pancreatic β-cells and has a functional role in exocytosis, Diabetes 49 (2000) 383–391.
[44] A. Gut, C.E. Kiraly, M. Fukuda, K. Mikoshiba, C.B. Wollheim, J. Lang, Expression and localisation of synaptotagmin isoforms in endocrine β-cells: their function in insulin exocytosis, J. Cell Sci. 114 (2001) 1709–1716.
[45] M. Iezzi, G. Kouri, M. Fukuda, C.B. Wollheim, Synaptotagmin V and IX isoforms control Ca^{2+}-dependent insulin exocytosis, J. Cell Sci. 117 (2004) 3119–3127.
[46] J. Lang, M. Fukuda, H. Zhang, K. Mikoshiba, C.B. Wollheim, The first C2 domain of synaptotagmin is required for exocytosis of insulin from pancreatic β-cells: action of synaptotagmin at low micromolar calcium, EMBO J. 16 (1997) 5837–5846.
[47] D.M. Thomas, G.D. Ferguson, H.R. Herschman, L.A. Elferink, Functional and biochemical analysis of the C2 domains of synaptotagmin IV, Mol. Biol. Cell 10 (1999) 2285–2295.
[48] Z.X. Wu, S. Xia, L. Xu, L. Bai, T. Xu, Dynamic imaging of single secretory granule in cultured PC12 cells, Acta Biochim. Biophys. Sin. 35 (2003) 381–386.
[49] T. Xu, M. Naraghi, H. Kang, E. Neher, Kinetic studies of Ca^{2+} binding and Ca^{2+} clearance in the cytosol of adrenal chromaffin cells, Biophys. J. 73 (1997) 532–545.
[50] G. Grynkiewicz, M. Poenie, R.Y. Tsien, A new generation of Ca^{2+} indicators with greatly improved fluorescence properties, J. Biol. Chem. 260 (1985) 3440–3450.
[51] H.S. Liu, Z.T. Hu, K.M. Zhou, Y.M. Jiu, H. Yang, Z.X. Wu, T. Xu, Heterogeneity of the Ca^{2+} sensitivity of secretion in a pituitary gonadotrope cell line and its modulation by protein kinase C and Ca^{2+}, J. Cell. Physiol. 207 (2006) 668–674.
[52] M. Iezzi, L. Eliasson, M. Fukuda, C.B. Wollheim, Adenovirus-mediated silencing of synaptotagmin 9 inhibits Ca^{2+}-dependent insulin secretion in islets, FEBS Lett. 579 (2005) 5241–5246.
[53] G. Nagy, J.H. Kim, Z.P. Pang, U. Matti, J. Rettig, T.C. Sudhof, J.B. Sorensen, Different effects on fast exocytosis induced by synaptotagmin 1 and 2 isoforms and abundance but not by phosphorylation, J. Neurosci. 26 (2006) 632–643.
[54] C. Heinemann, R.H. Chow, E. Neher, R.S. Zucker, Kinetics of the secretory response in bovine chromaffin cells following flash photolysis of caged Ca^{2+}, Biophys. J. 67 (1994) 2546–2557.
[55] C. Smith, E. Neher, Multiple forms of endocytosis in bovine adrenal chromaffin cells, J. Cell Biol. 139 (1997) 885–894.
[56] L. Eliasson, P. Proks, C. Ammala, F.M. Ashcroft, K. Bokvist, E. Renstrom, P. Rorsman, P.A. Smith, Endocytosis of secretory granules in mouse pancreatic β-cells evoked by transient elevation of cytosolic calcium, J. Physiol. 493 (Pt. 3) (1996) 755–767.